Lattice Boltzmann simulation on porous structure and soot accumulation

Kazuhiro Yamamoto [a,*], Shingo Satake [a], Hiroshi Yamashita [a], Naoki Takada [b], Masaki Misawa [b]

[a] *Department of Mechanical Engineering, Nagoya University*
Furo-cho, Chikusa-ku, Nagoya, Aichi 464-8603, Japan

[b] *National Institute of Advanced Industrial Science and Technology (AIST)*
16-1 Onogawa, Tsukuba, Ibaraki 305-8569, Japan

Abstract

In this study, using the lattice Boltzmann method, we simulate soot accumulation in porous media to examine the particle trap in a diesel particulate filter (DPF). The porous media are numerically formed for different inner structure with given porosity. The porous structure similar to the real sample, Ni-Cr metal, can be obtained, where the pressure fields in both cases are almost the same. In the simulation of soot accumulation, the velocity field is changed when the soot is attached to the porous wall. The pressure drop is largely increased. Interestingly, the friction factor is smaller than experimentally predicted value by Ergun equation.

Key words: Lattice Boltzmann method, Soot, Porous media, Diesel particulate filter
PACS: 47.11.-j, 47.55.Kf, 47.56.+r, 47.61.-k, 47.70.Fw

1 Introduction

Recently, the share of a diesel car in the world is gradually increased, because diesel engines have an advantage of low fuel consumption in comparison with gasoline engines. However, diesel exhaust gas has more ambient air pollutants such as oxides of nitrogen (NOx), carbon monoxide, carbon dioxide, unburned hydrocarbons, and particulate matters (PM) including soot [1]. These emissions are of concern for detrimental effects to human health and

* Tel. & fax : +81-52-789-4471
Email address: kazuhiro@mech.nagoya-u.ac.jp (Kazuhiro Yamamoto).

the environment, which contribute smog, acid rain, and global warming. Due to the public awareness with regard to harmful emissions, the governments are setting more strict exhaust emissions standards such as Euro V in 2008. In Japan, the Tokyo municipal government has begun to regulate diesel-powered commercial vehicles that fail to meet their new emission standards.

As one of the key technologies, a diesel particulate filter (DPF) has been developed to reduce PM in the after-treatment of exhaust gas. In simple explanation of DPF, it traps the particles when exhaust gas passes its porous structure. Since the filter would readily be plugged with particles in a short time, the accumulated particles must be removed. The trapped particles are chemically treated, and usually burned in combustion. This is called filter regeneration process. So far, it is difficult to observe the phenomena experimentally, and there may not be enough information to understand the particle accumulation in filters. Although it is a big advantage to simulate fluid flow in DPF, it is very challenging to deal with the phonemena in the filter by conventional computational code, because the particulate matters are very small (typically less than 10 microns) and we need to consider the small scale and complex geometry with chemical reaction. In the lattice Boltzmann method (LBM), the treatment of boundary conditions is simple and easy, and it is appropriate to calculate porous media flow [2-8]. Recently, we have simulated the flow in three-dimensional porous structure by LBM [9]. The soot reaction is included to consider the filter regeneration process.

Usually, DPF is a ceramic filter, and we need to test many trial products for more efficient DPF structure for PM trap. Since it costs a lot to manufacture filters, it is appropriate to obtain filter characteristics in advance by simulation. In our previous study, we have proposed an approach to form porous media structure numerically [10]. It is based on the simulation of self-aggregated fluids by Rothman and Keller model [11], and the complex geometry like porous media structure is produced. Although it is two-dimensional simulation by D2Q9 model, it is possible to choose freely the porosity and tortuosity of porous media. In this paper, we apply this aproach to three-dimensional simulation. To validate our scheme, we compare the simulated porous structure with the real sample, Ni-Cr metal [9]. Then, we simulate soot accumulation in porous media.

2 Numerical Method

We develop numerical scheme for simulating fluid with soot accumulation in porous media. The incompressible lattice BGK model of D3Q15 [5] is used. The soot accumulation is described by the modified particle deposition model [12]. Different from Lagrangian approach by the equation of motion [13], individual

particles are not considered. Instead, the soot concentration is monitored at the grid around the porous wall surface. As the soot accumulation is continued, the soot concentration becomes unity. When this limit is reached, the solid site is piling up. The accumulated soot region is treated as non-slip wall, which implies a dynamically change of boundary condition for fluid. The LB equation for soot mass fraction is,

$$F_{C,\alpha}(\mathbf{x}+\mathbf{e}_\alpha\delta_t, t+\delta_t) - F_{C,\alpha}(\mathbf{x},t) = -\frac{F_{C,\alpha}(\mathbf{x},t) - F^{eq}_{C,\alpha}(\mathbf{x},t)}{\tau_C} + w_\alpha Q_C \quad (1)$$

where F_C is the distribution function for soot mass fraction, δ_t is the time step, w_α=1/9 (α=1:6), w_α=1/72 (α=7:14), w_{15}=2/9, and τ_C is the relaxation time determined by diffusion coefficient. The source term, Q_C, is the treatment of soot accumulation around the porous wall surface. For simplicity, soot is thoroughly attached to the porous wall without desorption. The equilibrium distribution function, $F^{eq}_{C,\alpha}$, is given by

$$F^{eq}_{C,\alpha} = w_\alpha Y_C \left\{ 1 + 3\frac{(\mathbf{e}_\alpha \cdot \mathbf{u})}{c^2} + \frac{9}{2}\frac{(\mathbf{e}_\alpha \cdot \mathbf{u})^2}{c^4} - \frac{3}{2}\frac{\mathbf{u}\cdot\mathbf{u}}{c^2} \right\} \quad (2)$$

The mass fraction of soot is obtained by the sum of the distribution function as $Y_C = \sum_\alpha F_{C,\alpha}$.

Figure 1 shows the coordinate and boundary conditions. The calculation domain is 5 cm × 1 cm × 1 cm, and the inflow velocity, U_{in}, is 10 cm/s. The inlet length of L is 1cm of 40 grid length. The total number of grids is 201 × 41 × 41, with grid size of 0.25 mm. The porous structure of 100 grid length is placed in the center part in this figure. In the calculation, all equations are non-dimensionalized based on similarity to obtain the flow and concentration fields. As for the boundary condition, the inflow boundary is adopted at the inlet [14]. At the sidewall, the slip boundary condition is adopted, considering the symmetry [6]. At the outlet, the pressure is constant, and the gradient of soot concentration is zero. On the surface of the porous wall, bounce-back rule for non-slip boundary condition is adopted.

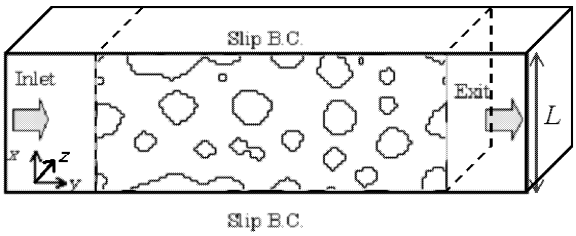

Fig. 1. Coordinate and boundary conditions in porous media flow.

3 Results and discussion

3.1 Porous structure

In Rothman and Keller model, the blue and red phases are calculated. As already simulated [10], it is considered that the blue phase is the region available for flow, and the red phase is porous media. Figure 2 shows time evolution of self-aggregation. The fraction of red phase in x-y plane is shown. Time steps (IT) are 50, 300, 1300, and 2000, respectively. The total density ratio of blue particles to red particles is about three, corresponding to the porosity of 0.75. At initial condition (IT = 0), particles for both phases are placed randomly. As seen in this figure, the phase separation is observed. At later time step, the red spot colligate each other to become larger spot. Resultantly, the surface of interface is decreased monotonically.

In theoretical consideration in porous media flow [15], the key parameters of porous structure are porosity and total wetted surface. These two parameters are shown in Fig. 3 to observe the time dependence. The wetted surface, S_w, is non-dimensionalized by the inlet area of L^2. It is clearly shows that only the wetted surface is decreased as the time step goes, while the porosity is almost unchanged. Then, in our approach, we can obtain different porous structure with porosity constant.

To validate our present model for porous media formation, we compare the simulated porous structure with the real sample, Ni-Cr metal. We use 3D-CT

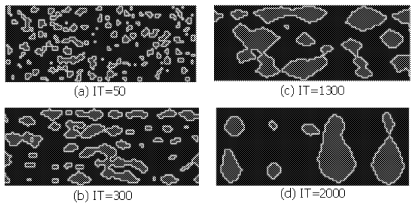

Fig. 2. Time evolution of self- aggregation at representative time steps.

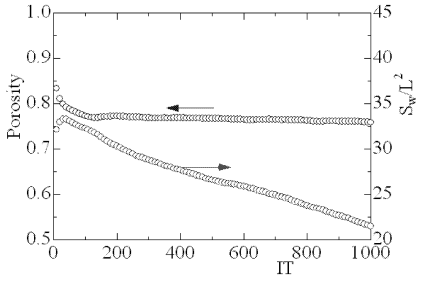

Fig. 3. Porosity and total wetted surface.

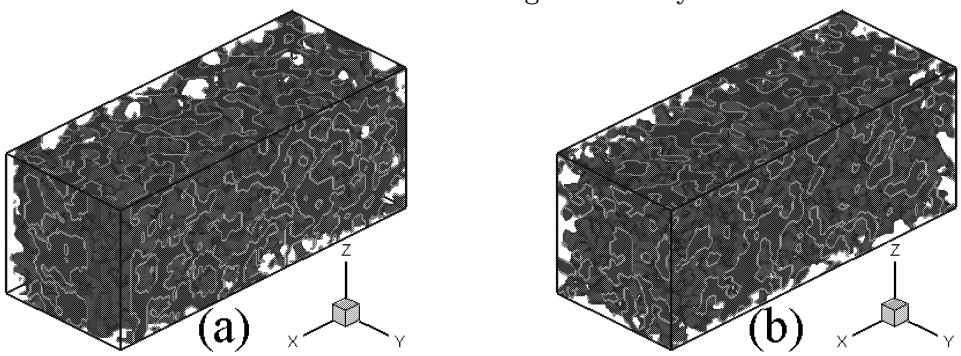

Fig. 4. Porous structure; (a) Ni-Cr metal, (b) simulated media in this study.

technique to calculate porosity and wetted surface [9]. The porous structure of Ni-Cr metal is shown in Fig. 4(a). The size is 4.3 mm $\times$ 1.7 mm $\times$ 1.7 mm with grid size of 43 μ m. The estimated porosity is 0.56, and the wetted surface is of $S_w/L^2 = 49$. We form the porous media whose porosity and wetted surface are equal to those of Ni-Cr metal, which is shown in Fig. 4(b).

Then, the fluid simulation is conducted. Since the sample is small, the inlet length, L, is 1.7 mm in this calculation. First, we check the porosity in x-axis (flow direction) in these media. Figure 5 shows the mean porosity in the y-z plane. The porous media is placed in the range of $x/L = 1.25$ to 3.75 in this figure, and the porosity is unity outside this region. Although the porosity is slightly changed due to non-uniformity of the porous structure, both profiles are almost the same. Figure 6 shows the pressure distribution in the steady state flow. The mean pressure in the y-z plane is shown, normalized by the constant pressure at the outlet. As seen in this figure, the pressure change is observed only in the porous region. It decreases almost linearly along the flow direction. To compare these two cases, it is found that the pressure profiles are almost the same. Then, we conclude that the porous structure similar to that of the real sample can be formed by our proposed approach.

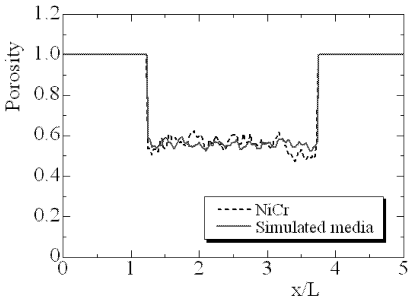

Fig. 5. Porosity of Ni-Cr metal and simulated media.

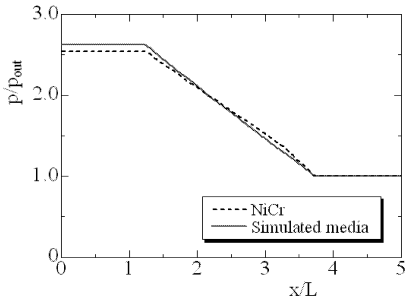

Fig. 6. Pressure distributions in Ni-Cr metal and simulated media.

3.2 Soot accumulation

Then, we simulate the flow with soot accumulation. Figure 7 shows soot concentration fields. These profiles are obtained at IT = 100 and 300. The mass fraction of soot at the inlet, $Y_{C,in}$, is 0.1, and the porosity of porous media is 0.9. After the soot is attached to the porous wall, the velocity field is changed. That is, the velocity is largely accelerated at the narrow path due to soot accumulation. The soot is preferably accumulated upstream. At the same time, the pressure drop becomes larger as the soot deposition proceeds. The similar pressure change is observed when the deposited layer is developed in the gas-particle flow [13].

To see the effect of soot accumulation on flow field, results are compared with the Ergun equation (Eq.(3)), which is the empirical equation in porous

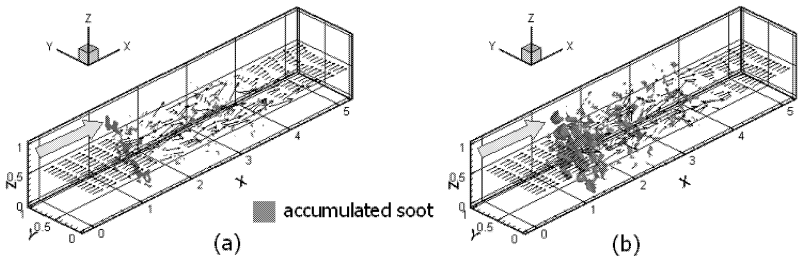

Fig. 7. Soot accumulation with velocity vector; (a) IT = 100, (b) IT = 300.

media flow [15].

$$f = \frac{150}{\mathrm{Re}} + 1.75 \ , \ \mathrm{Re} = \frac{U_{in} D_p}{\nu(1-\varepsilon)} \ , \ f = \left(-\frac{dp}{dx}\right) \frac{D_p}{\rho_0 U_{in}^2} \frac{\varepsilon^3}{(1-\varepsilon)} \quad (3), (4), (5)$$

Here, Reynolds number, Re, and friction factor, f, are called Ergun coordinates, and ε is the porosity. The pressure gradient is estimated in the porous region, and the equivalent diameter, D_p, is determined by the porosity and wetted surface. The inflow velocities are 1, 5, 10, 20 cm/s. Results at IT = 100, 200, 300, 400, 500, and 600 are shown in Fig. 8. The friction factor before soot accumulation is also plotted.

When soot is attached to the porous wall, the porosity is gradually decreased, with larger wetted surface. Resultantly, the Reynolds number in Eq. (4) is decreased. On the other hand, the friction factor after soot accumulation is smaller than the predicted value by Ergun equation, although both results show good agreement before soot accumulation. On the contrary, after IT = 300, the friction factor is steeply increased. As seen in Fig. 7, more soot is attached at the inlet side of porous region, where the steep pressure drop is observed. Needless to say, when the channel around the inlet is completely plugged with soot, there is no flow passing through the porous media. Hence, it is considered that the flow starts to be plugged with soot at IT > 300. In the derivation of the Ergun equation, the assumption of both steady flow and uniform porosity is adopted. Therefore, the discrepancy of friction factor is explained by the abrupt pressure change and unsteadiness of flow due to the

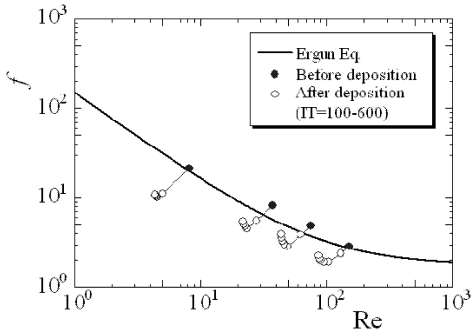

Fig. 8. Friction factor and Ergun equation.

non-uniform soot accumulation.

4 Conclusions

We have simulated soot accumulation in porous media. The porous structure is formed by the self-aggregated fluids. The simulated porous media has been compared with the real sample, Ni-Cr metal. The results show that:
(1) Porous media structure is freely produced based on profile of self-assembled binary mixture, and the structure similar to that of the real sample can be formed by our proposed approach.
(2) Soot accumulation is well simulated to observe effect of soot accumulation on flow field, with smaller porosity and larger wetted surface.
(3) The friction factor with soot accumulation is smaller than the predicted value by the Ergun equation.

Acknowledgements

This work was partially supported by Japan Society for the Promotion of Science under Grant-in-Aid for Scientific Research (No.17760162) and Mazda Foundation in Japan.

References

[1] R. A. Searles, D. Bosteels, C. H. Such, A. J. Nicol, J. D. Andersson, and C. A. Jemma, F02E310:1-17, *FISITA 2002 World Congress.*

[2] G. McNamara and G. Zanetti, Phys. Rev. Lett. **61** (1988) 2332.

[3] S. Succi, E. Foti and F. Higuera, Europhys. Lett. **10** (1989) 433.

[4] A. Cancelliere, C. Chang, E. Foti, D.H. Rothman and S. Succi, Phys. Fluids A **2** (1990) 2085.

[5] Y.H. Qian, D. d'Humie'res and P. Lallemand, Europhys. Lett. **17** (1992) 479.

[6] T. Inamuro, M. Yoshino, and F. Ogino, Int. J. Numer. Meth. Fluids **29** (1999) 737.

[7] J. Bernsdorf, G. Brenner, and F. Durst, Comput. Phys. Commun. **129** (2000) 247.

[8] M.Yoshino and T.Inamuro, Int. J. Numer. Meth. Fluids **43** (2003) 183.

[9] K. Yamamoto, N. Takada, and M. Misawa, Proc. Comb. Inst. **30** (2005) 1509.

[10] K. Yamamoto and N. Takada, Special Volume in Physica A **362** (2006) 111.

[11] D. H. Rothmann and J. M. Keller, J. Stat. Phys. **52**, Nos.1/2 (1988) 367.

[12] B. Chopard, A. Masselot, and A. Dupuis, Comput. Phys. Commun. **129** (2000) 167.

[13] O. Filippova, and D. H*ä*nel, Comput. Fluids **26** (1997) 697.

[14] Q. Zou and X. He, Phys. Fluids **9** (6) (1997) 1591.

[15] R. B. Bird, W.E. Stewart and E.N. Lightfoot, *Transport Phenomena*, Wiley, New York (1960).